Q. HUANG[1],✉
A.S. TAN[1]
J.M. TAN[1]
I.S. GOH[1]
Z.Z. DONG[2]
C.K. ONG[3]
T. OSIPOWICZ[3]

Effect of exposure to air on sheet resistance and phase composition of Co silicides annealed at a low temperature of 470 °C

[1] Thin Film Department, System on Silicon Manufacturing Pte. Ltd., 70 Pasir Ris Drive 1, Singapore 519527
[2] Department of Electrical Science and Technology, Huazhong University of Science and Technology, Wuhan 430047, P.R. China
[3] Department of Physics, National University of Singapore, 10 Kent Ridge Crescent, Singapore 119260

ABSTRACT Attention has been attracted to Co silicides due to their superior properties in deep-submicron integrated circuit technology. In this paper, the effect of exposure to air on the properties of Co silicides has been studied. Co films of 20-nm thickness were deposited onto polysilicon layers using Ar sputtering. After deposition, the samples were exposed to air at room temperature for different times, ranging from 0 to 48 h, before a rapid thermal annealing (RTA) at 470 °C. It is found that exposure to air significantly changes the sheet resistance (R_s) and the phase composition of the silicides. The sample exposed to air for 48 h has R_s of $\sim 71\ \Omega/\text{sq}$, which is about 10% lower than that for the sample annealed immediately. This is due to the fact that more Co_2Si phase and less $CoSi$ phase are formed in the former sample. The mechanism can be attributed to the gases in air (e.g. O_2), which contaminate the Co/Si interface and act as a kinetic barrier during the subsequent RTA. It has been demonstrated that gaseous contamination from air strongly influences the $CoSi_x$ phase transformation.

PACS 81.05.Je; 81.40.Ef; 81.30.-t

1 Introduction

As the ultra-large-scale integration (ULSI) technology is scaling down to deep-submicron feature sizes, great attention has been attracted to Co silicide [1]. The merits of Co silicide include its low resistivity and low formation temperature [1], good chemical stability [2] (no formation of Co and As/B dopant compound), good thermal stability [3] as well as line-width independence [4]. In comparison with other silicides, Co silicide is superior to Ti silicide in its line-width independence [4] and superior to Ni silicide in its good thermal stability [3]. Therefore, Co silicide is the preferred choice for $\leq 0.18\text{-}\mu\text{m}$ technologies. However, processing issues still exist such as the rough interface formation and high junction leakage, which become serious for ultra-shallow junctions. In this case, a better understanding of the phase-formation mechanism for Co silicides is required.

Van Gurp and Langereis [5] first studied the growth of $CoSi_x$ by thermal annealing. They found that at low anneal-

✉ E-mail: qiang.huang@philips.com

ing temperatures mainly Co_2Si and $CoSi$ are formed. $CoSi_2$ only starts to form at a temperature $T > 500\ °C$. Xia et al. [6] studied the thermodynamic driving force of $CoSi_x$ formation by an ion-mixing method. It was revealed that, thermodynamically, $CoSi$ is easier to form than Co_2Si, and $CoSi_2$ is most difficult to form. Miura et al. [7] studied the kinetics and the phase-formation sequence of $CoSi_x$ by normal thermal annealing. They found that $CoSi_x$ formation is kinetically restricted (diffusion-restricted) rather than thermodynamically controlled during annealing. In addition, they also found that the local Co/Si ratio plays a crucial role in determining the final silicide phase, which Vantomme et al. [8] termed 'concentration-controlled phase selection'. Recently, Goto et al. [9] observed the formation of $CoSi_x$ spikes during a Co/Si reaction, especially for the samples annealed at ~ 400 to $450\ °C$. It was indicated that a localized reaction exists between Co/Si, and a high junction leakage can be caused. This makes it interesting to study further the Co silicidation at low annealing temperatures. On the other hand, Li et al. [10] studied the effect of thermal desorption of the gaseous impurity (O_2, H_2O, etc.) after the wafers have been stored in air for about two months. They argued that gas impurities from thermal desorption have a stronger impact on silicidation than the impurities in the annealing ambient. In this sense, it is interesting to study the effect of exposure to air on Co silicidation. In this paper, we examined the effect of exposure to air on properties of $CoSi_x$ annealed at a low temperature of 470 °C. The samples were exposed to air during the interval between Co deposition and the subsequent rapid thermal annealing (RTA). An annealing temperature of 470 °C was chosen, mainly due to the fact that $CoSi_2$ can hardly be formed when annealed at $T < 500\ °C$ [5, 7], which simplifies the problem.

2 Experiments

Co films of ~ 20-nm thickness were deposited onto polycrystalline Si (poly-Si) layers using dc magnetron sputtering (AMAT Endura). The base pressure of the deposition chamber is $\sim 2.0 \times 10^{-8}$ Torr. The deposition was carried out at room temperature under an Ar pressure of ~ 2 mTorr. Prior to Co deposition, the poly-Si layer was pre-cleaned using HF vapor and the native oxide was removed by sputter-etch. A commercial high-purity ($> 99.999\%$) Co target was used.
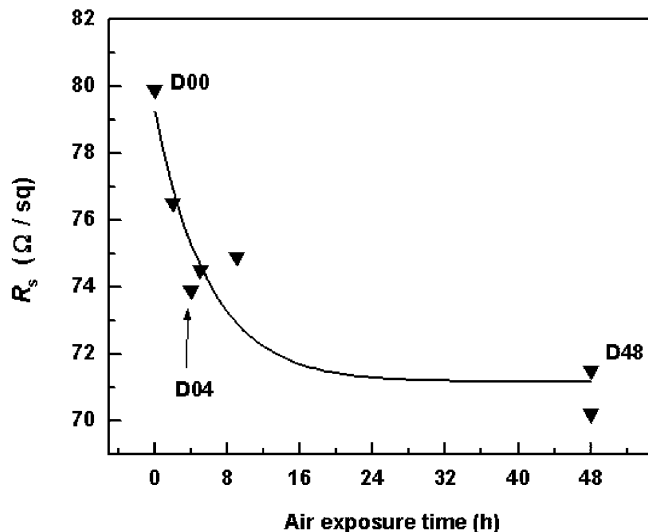
The substrates were *p*-type Si (100) wafers with a resistivity of 0.5–100 Ω cm. After the standard chemical cleaning, thermal oxide of 100 nm was grown and 200-nm-thick poly-Si was deposited using low-pressure chemical vapor deposition (LPCVD). After Co deposition, the samples were kept at room temperature in air (clean-room ambient) for a certain exposure time, ranging from 0 to 48 h. Then they were loaded into a RTA machine (AMAT Centura) and annealed at 470 °C for 60 s under a following N_2 ambient. The sheet resistance, R_s, of the samples was measured using the standard four-probe method by a RS-100. The microstructures of the samples were evaluated using X-ray diffraction (XRD), cross-section scanning electron microscopy (X-SEM), atomic force microscopy (AFM), microRaman spectroscopy and Rutherford backscattering spectrometry (RBS).
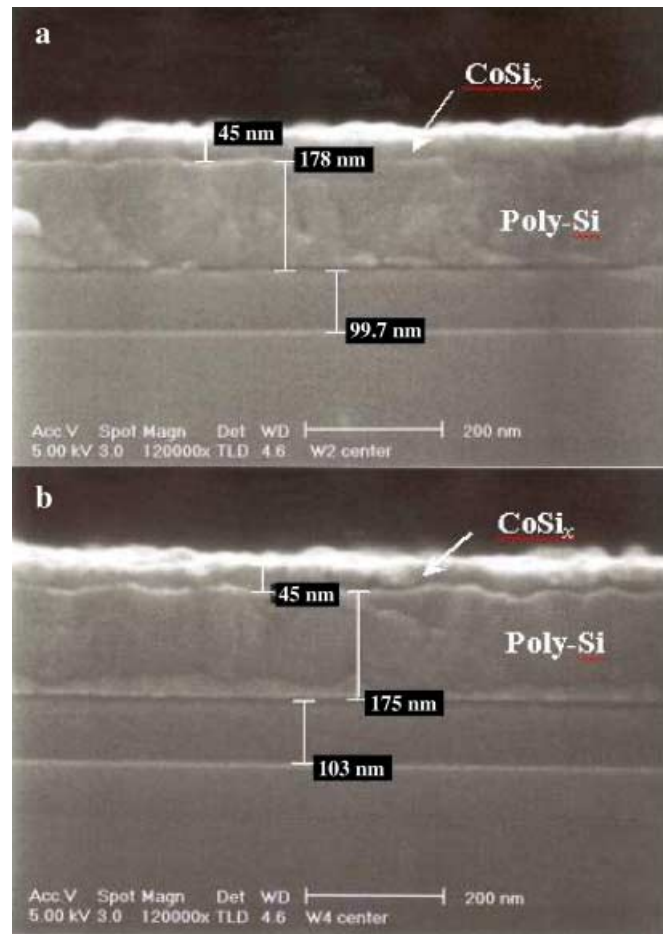
3   Results

Figure 1 presents the correlation between the sheet resistance R_s and the exposure time to air before RTA. A significant dependence of R_s on exposure time was found. Despite some scattering, a clear trend is seen: the samples with longer exposure times have lower R_s. For the samples with an exposure time of 48 h, R_s is around 71 Ω/sq, which is $\sim 10\%$ lower than that of the sample that was annealed immediately after Co deposition. To shed some light on the underlying mechanism, three samples, namely D00 (annealed immediately), D04 (4-h exposure time) and D48 (48-h exposure time) were selected for further microstructural characterizations.

X-SEM studies revealed that there is no significant change in the $CoSi_x$ film thickness, t, for the different samples. As an example, the X-SEM images of D00 and D48 are presented in Fig. 2. After RTA, t is around 45 nm for all samples. Due to the interface roughness, t ranges from 43.4 to 45 nm at different positions of a certain sample. For the sample with a longer delay time, the interface seems to be slightly rougher. Nevertheless, no apparent difference in silicide thickness t can be identified from sample to sample. In a four-point measure-

FIGURE 2   **a** The X-SEM images for the samples D00 and **b** that for the sample D48

ment [11],

$$R_s = C(\varrho/t), \tag{1}$$

where C is a geometrical factor and ϱ is the bulk resistivity. As t remains the same, it suggests that the changes in R_s observed in Fig. 1 originate mainly from the changes in ϱ.

Considering that ϱ can be influenced by microstructure features such as grain size, the surface morphologies of the samples have been checked by AFM, as shown in Fig. 3. Using a 'tapping' mode, both the magnitude and the phase images were recorded. The magnitude images (Fig. 3, left) reflect the surface morphologies, whereas the phase images (Fig. 3, right) reflect the surface-elasticity distributions. The silicide samples, D00, D04 and D48, show no apparent difference in morphology. All samples show an average grain size of ~ 35 nm and the grains are randomly distributed. Hence, the resistivity change in D48 cannot be due to the grain-size effect. On the other hand, a great change in the elasticity phase distribution has been identified. D00 apparently has two elastic phases, in contrast with D48 that has only one elastic phase. This suggests that the samples might have different chemical phase compositions. However, as AFM only characterizes the surface, the samples have to be further checked by XRD, Raman spectroscopy and RBS to determine the bulk phase compositions.
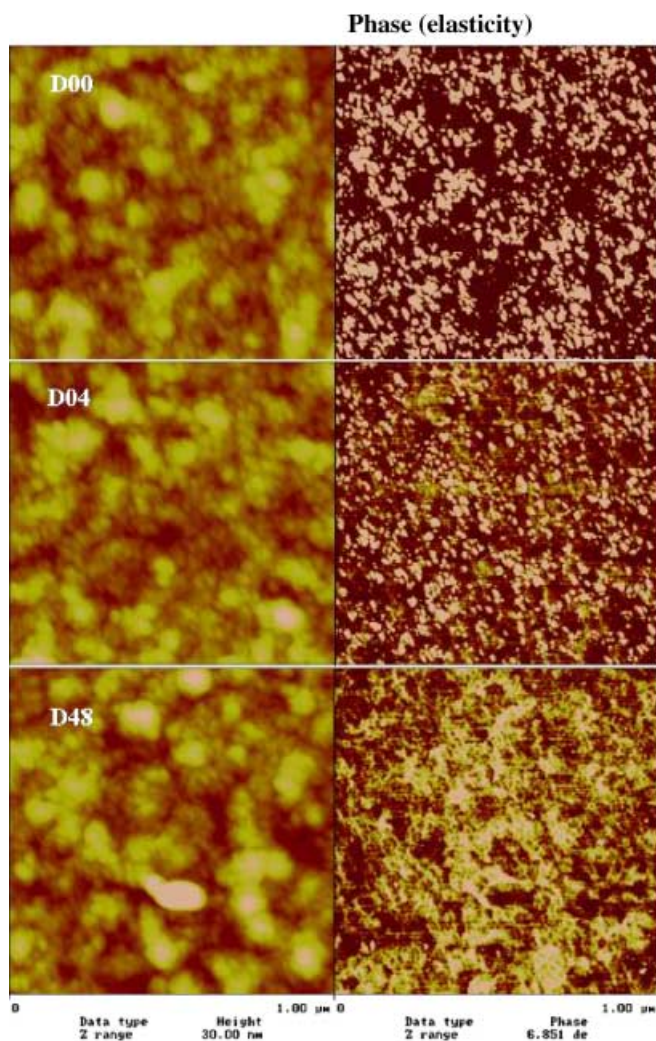

FIGURE 1   The sheet resistance for the $CoSi_x$ samples that were annealed at 470 °C for 60 s. The samples were exposed to air from 0 to 48 h before RTA

Phase (elasticity)

FIGURE 3   AFM images for the samples D00, D04 and D48. Both the surface morphologies (*left*) and the elasticity phases (*right*) have been shown
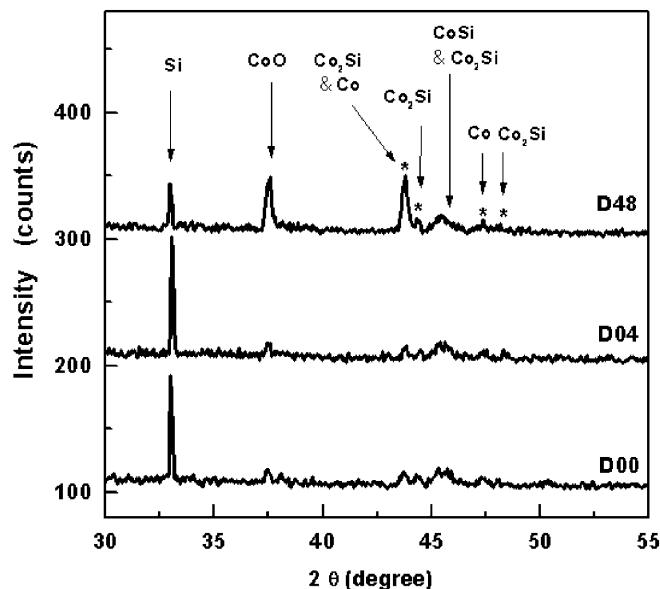

FIGURE 4   The XRD patterns of the as-prepared $CoSi_x$ samples
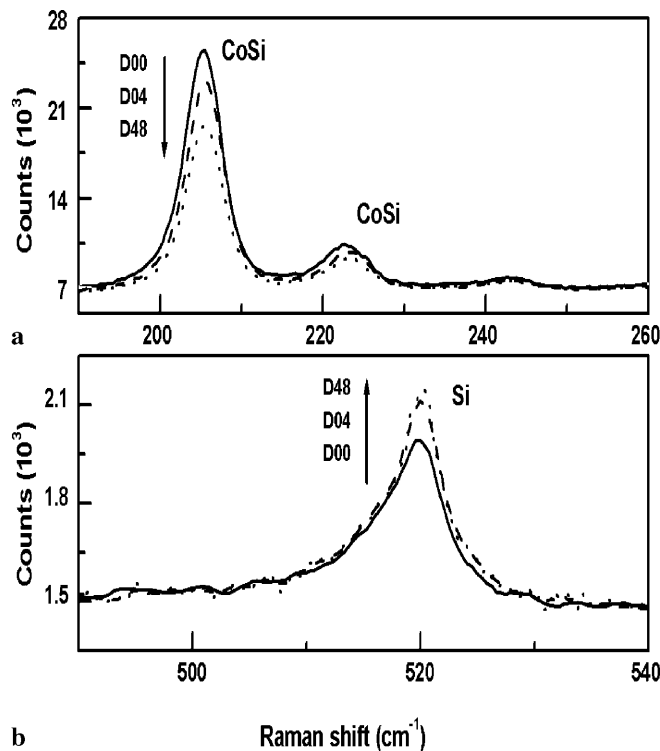
FIGURE 5   Raman spectrum for the as-prepared $CoSi_x$ samples. The measuring range is from 190 to 590 cm^{-1}

Figure 4 presents the XRD θ–2θ patterns of the Co silicide samples. The peaks are indexed according to the Powder Diffraction File: PDF-2 database [12]. It reveals that the silicide samples are polycrystalline and consist of multiple phases such as Co_2Si, CoSi, Co and CoO. The Si peaks in the figure come from the poly-Si underlayer. The Co_2Si and Co reflection peaks overlap at $2\theta = 43.95°$. The Co_2Si and CoSi peaks are both located at around $2\theta = 45.57°$ and cannot be resolved. Due to those peak overlaps, it is hard to tell the intensity changes for each individual phase. However, a careful examination reveals that the peaks around $45.57°$ (Co_2Si and CoSi) remain almost unchanged. In contrast, the peaks from the Co-rich phases (Co_2Si or Co) increased in D48, as marked using star symbols on the pattern. Here Co or Co_2Si are considered to be Co-rich as compared to CoSi. On the other hand, the CoO peak is also enhanced in D48. This indicates that more Co-rich phases and CoO are formed in the sample with a longer exposure time to air.

Figure 5 presents the Raman spectra of the samples. The measurement was taken in the range of 190–590 cm^{-1}. In this range, Si has a peak around 520 cm^{-1} and CoSi has two peaks around 205.4 cm^{-1} and 222.8 cm^{-1} [13]. No character-

istic Raman peak can be found for the Co_2Si phase [13]. It is worth noting that the highest CoSi peak is shown for D00, which has zero exposure time before RTA. As the exposure time increases, the CoSi peak is systematically lowered. For the sample with the longest exposure time (D48), the CoSi peak is lowest. On the other hand, the Si peaks show a trend that is contrary to the CoSi peaks, i.e. the higher the CoSi peak, the lower the Si peak. This is reasonable since only CoSi and Co_2Si phases are formed during the 470 °C anneal and the formation of the CoSi phase consumes more Si than the for-

mation of the Co_2Si phase. The above Raman spectra agree with the earlier XRD results. It suggests that the sample with longer exposure time (D48) contains not only more Co-rich (Co or Co_2Si) phase, but also less Si-rich (CoSi) phase.

Figure 6a presents the RBS spectra for the samples that were measured using a 2 MeV He^+ beam and a 50-mm^2 passivated implanted planar silicon (PIPS) detector, located at 112 degrees, together with simulations using the RUMP computer code [14]. The depth profiles used in generating the simulations are shown in Fig. 6b. It is seen that D00 has a more uniform depth distribution both for Co and Si elements. In contrast, D48 shows a stronger decrease in Co content and an increase in Si content in the direction from film surface to substrate. Previously, it was shown that the phase formation of the Co silicide is kinetically restricted [7]. Thermodynamically, CoSi is the first phase to be formed upon thermal annealing. However, after CoSi-phase formation, if excess Co exists, Co_2Si will be formed at a temperature of $\sim 350\,°C$; if excess Si exists, $CoSi_2$ will be formed at a temperature of $\sim 500\,°C$. As the silicide samples in this experiment were annealed under $470\,°C$, the formation of $CoSi_2$ can be ignored. On the other hand, the formation of the CoSi phase
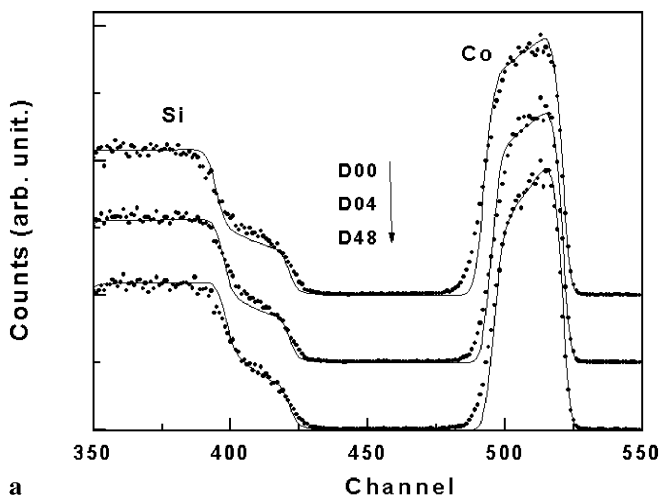
or the Co_2Si phase will depend on the local Co/Si atomic ratios (concentration-controlled phase selection) [7, 8]. The local Co/Si atomic ratios presented in Fig. 6b clearly suggest that more Co_2Si phase and less CoSi phase are formed in D48.
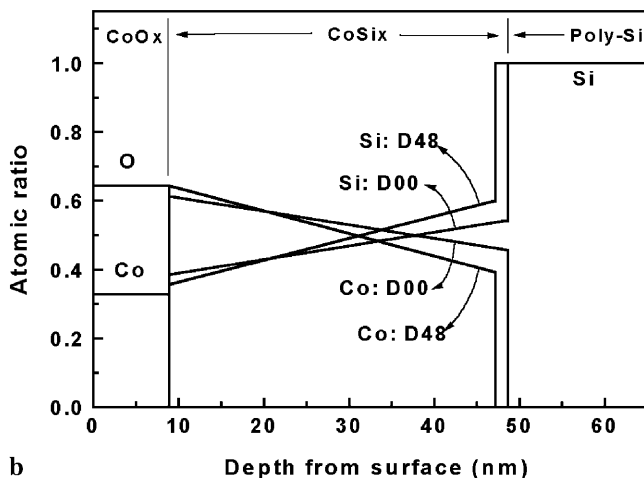
4   Discussion

According to the results in Sect. 3, the R_s change due to time delay is not caused by either the silicide film thickness change or the grain-size change. Instead, it is closely related to the phase composition of the samples. In Table 1, the phase composition of the Co silicide films is summarized in a qualitative manner. For a low-temperature annealing at $470\,°C$, silicide phases mainly consist of Co_2Si and CoSi components, whereas the formation of $CoSi_2$ is negligible. On the other hand, the CoO phase is also present due to the easy oxidization of Co. CoO can be formed either during a stay in air or during RTA.

Two main factors can influence R_s: (i) the variation in volume fraction of CoO phase at the film surface and (ii) the variation in volume fractions of Co_2Si and CoSi phases in the bulk film. The bulk resistivities of Co_2Si, CoSi and $CoSi_2$ are $\sim 40\,\mu\Omega\,cm$, $\sim 150\,\mu\Omega\,cm$, and $\sim 18\,\mu\Omega\,cm$, respectively [15]. CoO has a much higher resistivity $\varrho_{CoO} > 10\,000\,\mu\Omega\,cm$. We noted that $\varrho_{CoO} \gg \varrho_{CoSi_x}$, where ϱ_{CoSi_x} denotes the resistivity of silicide phases Co_2Si, CoSi and $CoSi_2$. If we assume that the contribution from CoO to R_s dominates, we expect that D48 has the highest R_s, because it was exposed to air for the longest period and has the most pronounced CoO peak in the XRD pattern. However, this is in contrast with the experimental observation that D48 has the lowest R_s. Therefore, differences in CoO, if any, cannot make a major contribution to the R_s differences between the samples. This may be due to the fact that the four electrical probes can punch through the surface CoO layer and directly connect to the Co silicide layers during the R_s measurement. As the first factor has been ruled out, the second factor should be responsible for the R_s change in Fig. 1, i.e. the sample with the longer exposure time has a lower R_s because less CoSi (high resistivity) and more Co_2Si (low resistivity) are formed in them.

As for why less CoSi is formed in the samples with a long exposure time, the underlying mechanism can be understood by an interfacial diffusion barrier model, as shown in Fig. 7. It is suggested that interface reactions occur when the samples are exposed to air. Since the reaction rate is low at room temperature, the reacted area develops depending on the exposure time. Immediately after Co deposition, there is no interface reaction (Fig. 7a); after a certain exposure time, scattered regions are formed by localized interface reactions (Fig. 7b)


FIGURE 6   **a** The RBS spectrum for the $CoSi_x$ samples. The *scattered points* represent the experimental data. The *solid lines* are RUMP simulations. **b** The resultant depth profiles for D00 and D48

	Exposure time to air (h)	CoO	Co_2Si	CoSi	$CoSi_2$
D00	0	Less	Less	More	Negligible
D04	4	Less	Less	More	Negligible
D48	48	More	More	Less	Negligible
Resistivity ($\mu\Omega$ cm)		> 10 000	~ 40	~ 120	~ 18

TABLE 1   A qualitative description of the phase composition of the Co silicide films. The resistivity of each phase [15] is also shown
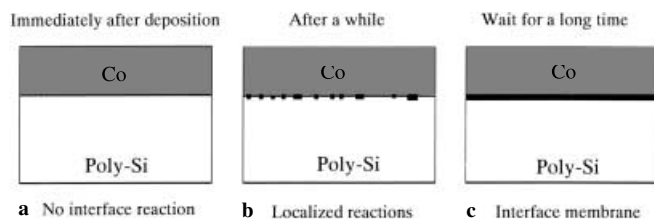
FIGURE 7   A simple illustration of the interfacial diffusion barrier formation sequence. **a** immediately after deposition, **b** after a while and **c** wait for a long time

and when the exposure time is long enough, the scattered regions collapse and form a continuous interface membrane (Fig. 7c). The reacted regions, or the membrane, act as a diffusion barrier for Co/Si atoms and influence the interdiffusion depth profile during RTA. According to this picture, D48 will have an interface membrane due to the long exposure time of 48 h. The membrane hampers the interdiffusion between Co/Si, causing Co and Si atoms to be less evenly distributed in D48 (see Fig. 6b). Considering that $CoSi_x$ phase formation depends on the local Co/Si atomic ratio, this results in less CoSi phase being formed in D48. In addition, the diffusion barrier may also affect the interface roughness. As revealed in Fig. 2, D48 has an apparently rougher interface than D00. This can be explained by the fact that the atom flux will first pass through the relatively weak points of the barrier during RTA, causing a rougher interface. Interestingly, Sarkar et al. [16] recently used a similar barrier picture to study the reactive deposition of $CoSi_2$. They suggested that the growing $CoSi_2$ layer at the Co/Si boundary serves as an instantaneous barrier for Co/Si diffusion. The interface roughness and the silicide quality are influenced by the barrier. In our experiment, the samples were exposed to air at room temperature; therefore, the Co/Si reaction should not occur (Co/Si reacts only when $T > 200\,°C$) [7]. However, Si tends to react with O_2 or gaseous H_2O at room temperature. According to Li et al. [10], the change of free energy ΔG is around $-850\,kJ/mol$ for the $Si + O_2$ reaction, but is only around $-100\,kJ/mol$ for the $Co + Si$ reaction. During the exposure to air, the gaseous impurities can diffuse along the grainboundaries (GBs) of the films and the SiO_x reaction occurs at the interface, as shown in Fig. 7. The resulting SiO_x will act as a barrier during RTA and affect the $CoSi_x$ phase formation.

To confirm the role of gaseous contamination from air, one more sample, V48, was prepared using the same conditions as D48 except that it was stored in high vacuum (at the base pressure of the deposition chamber for 48 h). If the interfacial barrier is formed mainly due to the Co/Si reaction, V48 will have a lower R_s than D00. However, V48 showed a R_s of

$\sim 80\,\Omega/sq$, similar to that of D00. This confirmed that it is the gaseous contamination during exposure to air that affects the final phase formation.

5   Conclusions

The effect of exposure to air on properties of Co silicide has been carefully examined. At a low annealing temperature of $470\,°C$, the resultant silicide films are composed of multi-phases, such as CoSi, Co_2Si, CoO, etc. Exposure to air before RTA significantly changes the sheet resistance and the phase composition of the silicides. The sample with a long exposure time of 48 h has R_s of $\sim 71\,\Omega/sq$, which is about 10% lower than that for the sample annealed immediately. This is due to the fact that more Co_2Si phase and less CoSi phase are formed in the former sample, as revealed by Raman and RBS analysis. On the other hand, as exposure time increases, the $CoSi_x$/Si interface also becomes rougher. The mechanism can be attributed to the gases in air (e.g. O_2) that contaminate the Co/Si interface, acting as a kinetic barrier during the subsequent RTA. The above picture is further supported by the fact that the sample stored in high vacuum for 48 h has a similar R_s to the sample annealed immediately. It has been shown that gaseous contamination from air has a significant effect on the $CoSi_x$ phase transformation.

REFERENCES

1 J.A. Kittl, W.T. Shiau, Q.Z. Hong, D. Miles: Microelectron. Eng. **50**, 87 (2000)
2 K. Maex, R. De Keersmaecker, G. Ghosh, I. Delaey, V. Probst: J. Appl. Phys. **66**, 5327 (1989)
3 T. Ohguro, M. Saito, E. Morifuji, T. Yoshitomi, T. Morimoto, H.S. Momose, Y. Katsumata, H. Iwai: IEEE Trans. Electron Devices **47**, 2208 (2000)
4 K. Maex: Mater. Sci. Eng. **R11**, 53 (1993)
5 G.J. van Gurp, C. Langereis: J. Appl. Phys. **46**, 4301 (1975)
6 W. Xia, C.A. Hewett, M. Fernandes, S.S. Lau, D.B. Poker: J. Appl. Phys. **65**, 2300 (1989)
7 H. Miura, E. Ma, C.V. Thompson: J. Appl. Phys. **70**, 4287 (1991)
8 A. Vantomme, S. Degroote, J. Dekoster, G. Langouche, R. Pretorious: Appl. Phys. Lett. **74**, 3137 (1999)
9 K. Goto, A. Fushida, J. Watanabe, T. Sukegawa, Y. Tada, T. Nakamura, T. Yamazaki, T. Sugii: IEEE Trans. Electron Devices **46**, 117 (1999)
10 H. Li, G. Vereecke, K. Maex, L. Froyen: J. Electrochem. Soc. **148**, G344 (2001)
11 A. Uhlir: Bell Syst. Tech. J. **34**, 105 (1955)
12 Powder Diffraction File: PDF-2 database [computer file], International Center for Diffraction Data, 1996–2000
13 H. Ying, Z.H. Wang, D.B. Aldrich, D.E. Sayers, R.J. Nemanich: Mater. Res. Symp. Proc. **320**, 335 (1994)
14 L.R. Doolittle: Nucl. Instrum. Methods B **9**, 344 (1985)
15 A. Appelbaum, R.V. Knoell, S.P. Muraka: J. Appl. Phys. **57**, 1880 (1985)
16 D.K. Sarkar, I. Rau, M. Falke, H. Giesler, S. Teichert, G. Beddies, H.-J. Hinneberg: Appl. Phys. Lett. **78**, 3604 (2001)